Analysis and Optimization of MirrorSAR Synchronization

Nertjana Ustalli, Gerhard Krieger, Josef Mittermayer, and Michelangelo Villano
German Aerospace Center (DLR), Microwaves and Radar Institute, Germany

Abstract

Phase synchronization poses a significant challenge for multistatic synthetic aperture radar (SAR) systems. A novel concept, called MirrorSAR, has been introduced, which relies on a configuration of transmitter and receiver satellites positioned at separate locations. In this setup, the receiver satellites serve as mirrors or space transponders, redirecting the radar echoes back to the transmitter. This configuration simplifies the receiver functionality and enables the utilization of cost-effective platforms. Within the transmitter, the forwarded radar signals are coherently demodulated using the same oscillator responsible for generating the radar pulses. This eliminates the need for a bidirectional phase synchronization link between the transmitter and receiver, as done in TanDEM-X, thus allowing for innovative synchronization approaches that guarantee the desired bistatic and interferometric performance, while keeping the receiver complexity low. This paper addresses in detail this phase synchronization approach and introduces optimized implementation aspects. The phase synchronization accuracy is assessed through simulation based on interferometric TanDEM-X data. Residual phase synchronization errors smaller than 1° are achieved for typical oscillators.

1 Introduction

Synthetic aperture radar (SAR) is a remote sensing technology widely utilized for Earth observation applications. In recent times, there has been a growing interest in the development of bi- and multistatic SAR systems, involving the deployment of separate transmit and receive antennas on distinct platforms [1]. Multistatic SAR systems offer new opportunities over their monostatic counterparts, including frequent monitoring, high-resolution wide-swath imaging, improved scene classification through bistatic imaging, generation of high-resolution digital elevation models (DEMs) with decimeter-level height accuracy through multibaseline cross-track interferometry, SAR tomography, as well as enhanced flexibility and reliability. However, the implementation of these systems poses new challenges that require attention, such as collision avoidance within closely spaced satellite formations, orbit design for establishing appropriate baselines, instrument synchronization involving time, space, and phase synchronization, as well as considerations for cost reduction [2] – [3]. Among the mentioned challenges, phase synchronization is one of the most critical. In bi- and multistatic SAR systems, the radar oscillators are physically separated and, as a result, the relative frequency deviation and phase noise between the transmitting and receiving oscillators cannot be canceled, unlike in monostatic SAR systems that use the same oscillator for modulation and demodulation. Uncompensated phase errors in bistatic SAR systems can lead to several undesired effects, including distortions in bistatic SAR focusing, such as time-variant shifts, spurious side lobes, and broadened impulse responses, as well as low-frequency phase modulation in the focused SAR image. Additionally, these errors can introduce interferometric phase errors, which may result in low-frequency modulations of the DEM along the azimuth direction [4].

The stringent requirements for interferometric phase stability will require relative phase referencing between the independent ultrastable oscillators. In recent years, several studies on phase referencing for bistatic SAR systems have been published. The concept of employing a continuous duplex satellite links with an ultrastable local-oscillator signal to compensate for oscillator drift was first proposed in [5]. An alternative synchronization approach involving pulsed alternates was suggested in [6] and effectively employed in the TanDEM-X mission [7]. Another approach to address the need for relative phase referencing involves the utilization of hyperstable oscillators combined with ground control points [4].

MirrorSAR, a new SAR system concept proposed in [8], consists of a set of spatially separate transmit and receive satellites and employs a fractionated radar architecture to reduce the complexity, weight, and power demands of the receiver hardware. MirrorSAR is a promising technique for implementing low-cost yet high-performance multistatic SAR missions, such as those being developed in the context of NewSpace. It can be operated in various modes, including single-transmit single-receive mode, single-transmit multiple-receive mode (as shown in **Figure 1**), or even multiple-transmit multiple-receive mode. The scene is illuminated by the transmitting satellite and the backscattered radar signals received by the receiving satellites are forwarded towards the transmitter through a phase preserving link. The routed radar signals are then demodulated to baseband by using, for example, a coherent I/Q demodulator driven by the local oscillator of the transmitter. Since this oscillator has also been used to generate the transmitted radar pulse, possible frequency and phase drifts are canceled, as in a classical monostatic SAR.

During its Phase 0/A, the Microwaves and Radar Institute of DLR proposed to extend the HRWS mission [9] with three small and low-cost receive-only satellites based on the MirrorSAR concept. The MirrorSAR concept will enable the acquisition of multiple large and small Rx baselines at the same time, allowing for highly accurate and robust SAR interferometry. The goal of the mission is to provide a global X-band DEM with a height accuracy of 2 m (point-to-point error, 90 % confidence interval) and horizontal posting of 4 m × 4 m [9].

An important aspect of MirrorSAR is bistatic radar signal synchronization. Two different synchronization approaches were proposed in [8] with the goal to keep the MirrorSAR receiver complexity low and still guarantee the bistatic and interferometric performance.

One of the synchronization options considers the use of a modulation that preserves the phase of the routed radar signal and avoids any dependency on the phase of the modulation carrier. For instance, the receiver satellite generates a high frequency signal, which can be either microwave or an optical carrier. This signal is then amplitude modulated by the radar echo before being forwarded to the transmitter. A simple amplitude demodulation at the transmitter can recover the time-delayed radar echo without phase disturbance from the high frequency carrier. Afterward, the radar echoes are demodulated to baseband using the same oscillator used to generate transmitted radar pulses. An alternative solution for achieving the required phase synchronization, instead of using an optical link, is the utilization of a microwave link. In this approach, a synchronization signal is transmitted from the transmitting satellite towards the receiving satellites by using a dedicated low-gain antenna. The received synchronization signal is superimposed to the radar echo on the receiving satellite. Subsequently, it is forwarded to the transmitter satellite, where the demodulation to baseband is performed by using the same oscillator used to generate transmitted radar pulses. This approach ensures that any additional phase error introduced on either the receiver and transmitter side will be identical for both the mirrored synchronization signal and the radar echo. An evaluation of the synchronization signal will allow for the compensation of these phase errors in the radar echo.

The approach based on the microwave link still leaves some open issues:

(i) Synchronization signal: The synchronization signal received by the Rx satellite should be weaker than the radar echo from the ground in order to avoid corrupting the radar echo data, while still ensuring phase error estimation with an accuracy of less than 1° for interferometric applications.

(ii) Removal of the synchronization signal: The removal of the synchronization signal should have minimal to no impact on the radar echo from the ground.

In light of the aforementioned challenges, this paper improves the phase synchronization approach based on a microwave link by introducing some novel implementation aspects, such as a pulse-to-pulse phase modulation to shift the synchronization signal outside the processed Doppler bandwidth, and assessing the performance for typical oscillators.

2 Phase Synchronization via Microwave Link

In this section we describe the processing steps performed to convert the data into a phase-corrected radar echoes suitable for SAR and interferometric processing. An overview of these processing steps is provided in **Figure 2**, where two panels are depicted that represent what is happening 'on-board' and 'on-ground'. We will introduce the fundamental building blocks of each part. Afterward, each block of the synchronization concept will be refined in greater depth.

The on-board synchronization for the case of a bistatic SAR system is shown in the upper panel of **Figure 2**. A synchronization signal is sent from Tx satellite to the Rx satellite. The synchronization signal is received in the Rx satellite by a dedicated antenna and superimposed then to the radar echo. In the Rx satellite, the overlaid signals are jointly frequency shifted by $+\Delta f$ using a coherent mixer and then radiated back to the transmitter. The superimposed shifted signal is received by the Tx satellite. Then, the additional frequency shift is reversed before the signal is down converted to baseband using the transmitter's local oscillator (LO). Finally, the baseband signal that is the sum of the radar echo and synchronization signal is digitized, stored in memory, and transmitted to the ground.

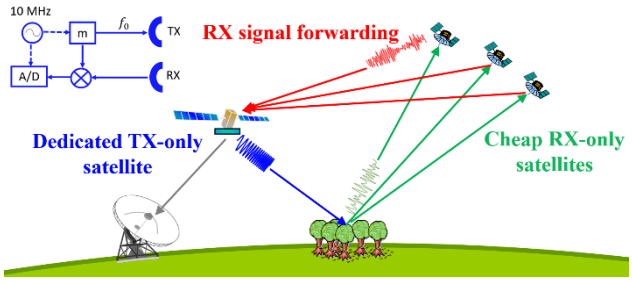

Figure 1 Illustration of the Mirror-SAR concept operating in single-transmit multiple-receive mode. The scene is illuminated by the Tx satellite. The scattered radar waves are then received by Rx satellites that route their recorded signals to the transmitter. The Tx satellite then coherently demodulates the forwarded signals before transferring them to the ground.

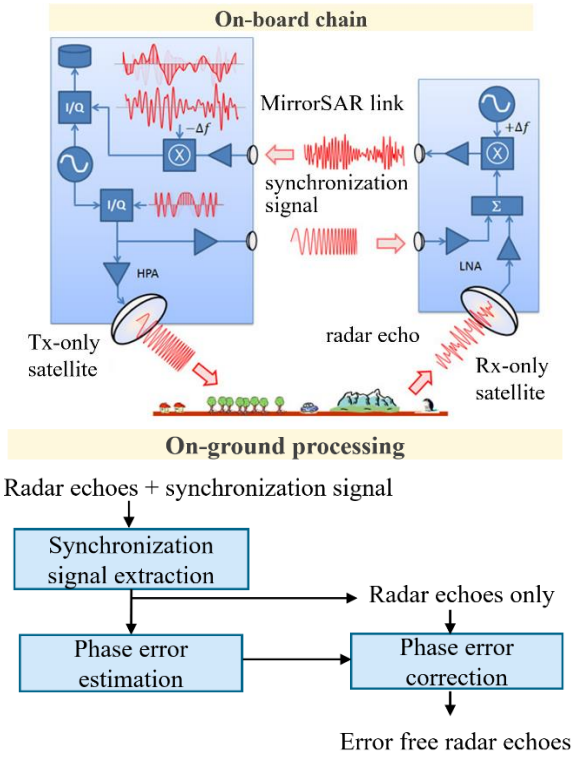

Figure 2 Main building blocks of the microwave link-based synchronization approach: (upper panel) on-board and (bottom panel) on-ground.

The superimposed synchronization signal and radar echo must be separated on the ground. It should be noted that the independent Rx satellite up conversion, i.e., $+\Delta f$, and the Tx satellite down conversion, i.e., $-\Delta f$ (see upper panel of **Figure 2**) introduce phase errors. However, these phase errors are the same for both the mirrored synchronization signal and the radar echo. As a result, after separating the synchronization signal from the radar echoes, an evaluation of the synchronization signal allows for the estimation and subsequently correction of these phase errors on the radar echo, as illustrated in the bottom panel of **Figure 2**. The synchronization signal will be removed from the radar echoes while attempting not to impact them.

Each component of the synchronization technique will now be discussed in greater depth, along with challenges and potential solutions.

2.1 On-board chain

The synchronization signal transmitted from Tx satellite towards Rx satellite can be a copy of the radar pulses sent to ground or a dedicated waveform that is coherently derived from the transmitters ultra-stable oscillator. In the following section, we will examine the performance in two scenarios: one, where the synchronization signal is a replica of the chirp transmitted to the ground (both being down chirp signals) and another, where the transmitted pulse and the synchronization signal are up- and down-chirps, respectively. It is important to note the synchronization signal will be weaker than the received radar echo. For every transmitted pulse on the ground we transmit a synchronization signal towards the Rx satellite with an additional delay (e.g., via a delay line or, more simply, by a cable whose length exceeds the final range resolution) in order to avoid potential interferences between the radar pulse sent to the ground and the much weaker synchronization signal sent to the receiver [8]. This interference could distort and shift the phase of the synchronization signal. Moreover, we propose a pulse-to-pulse phase modulation of the synchronization signal with a linear phase term. This modulation will shift the synchronization signal outside the processed Doppler bandwidth without impacting the radar echoes after its removal on the ground.

The synchronization signal will be received by the Rx satellite after a time delay that depends on the distance between the Tx and Rx satellite and the radar echo from the ground will be received after a time delay that depends on the bistatic range. Due to the different time delays a number of pulses equal to the number of traveling pulses (the number of pulses transmitted before the echo of any given pulse is received) will only have the synchronization signal returns, so these pulses will be shifted in frequency of $+\Delta f$ and forwarded to the Tx satellite without the superimposed radar echo returns.

The up-conversion, i.e., $+\Delta f$, and the down-conversion, i.e., $-\Delta f$ (see upper panel in **Figure 2**), are performed by independent oscillators resulting in phase errors. The instantaneous phase of an oscillator can be modelled as [10], [11]:

$$\varphi_{osc}(t) = 2\pi f_{osc} t + \varphi_{st}(t) + \varphi_0, \qquad (1)$$

where f_{osc} is the frequency of the oscillator (or its expected value, since the frequency itself is a random variable), φ_0 is a constant arbitrary phase and $\varphi_{st}(t)$ is a time-varying phase error. This phase error, also known as phase noise, is a random process and is often modelled by a second-order stationary stochastic process, which is conveniently characterized in the Fourier frequency domain by its power spectral density (PSD), $S_{\varphi_{st}}(f)$, where f is the frequency offset from f_{osc} [4]. Based on (1) the phase errors on the Tx side after the frequency shift reversing, (i.e., $-\Delta f$), can be modelled as:

$$\varphi_e(t) = 2\pi\delta f t + M\varphi_{st_{Tx}}(t) - M\varphi_{st_{Rx}}(t - \Delta t_{Rx-Tx}), \qquad (2)$$

where δf indicates a frequency offset produced by non-identical stable local oscillators (STALO) frequencies, $M = \Delta f / f_{osc}$ is the ratio of RF to master oscillator frequency, Δt_{Rx-Tx} is the time delay in the MirroSAR link (see upper panel of **Figure 2**), i.e., between the transmission of the superimposed signals from Rx satellite and their reception by the Tx satellite, $\varphi_{st_{Tx}}(t)$ and $\varphi_{st_{Rx}}(t - \Delta t_{Rx-Tx})$ are the random phase errors of the Tx satellite and Rx satellite oscillators at time t and $t - \Delta t_{Rx-Tx}$, respectively. Assuming uncorrelated master oscillators on the Tx and Rx satellites with equal PSD, $S_{\varphi_{st}}(f)$ and we can model the last two addends in (2) as a random process with PSD equal to $2MS_{\varphi_{st}}(f)$. It is important to notice that these phase errors will be the same for the synchronization signal and the radar echo, as the up-conversion $+\Delta f$ and down-conversion $-\Delta f$ is applied to the superimposed signal.

The overlaid signal is then down-converted to baseband using the same LO that generated the transmitted radar pulses. Due to a filtering effect known as range correlation, the low-frequency components of the phase noise of the LO are cancelled, similar to monostatic SAR systems. This filtering effect behaves as high pass filter and is caused by correlation between the phase noise on the LO signal and the phase noise on the received signal. The amount of filtering (i.e., the degree of correlation) is determined by the time delay between the transmitted and received signals and is greater at short time delays. As mentioned earlier, the time delay associated with receiving the synchronization signal, dependent on the two-way distance between the Rx and Tx satellites, differs from the time delay of the radar echo, dependent on the bistatic range. Consequently, the extent of low-frequency components canceled for the synchronization signal differs from that for the radar echo. However, it is important to note that this effect is negligible when compared to $\varphi_e(t)$ in (2). Therefore, we can conclude that the total phase errors on the synchronization signal and radar echoes, caused by the oscillators involved following demodulation to baseband, are equivalent to $\varphi_e(t)$.

2.2 On-ground processing

The retrieval of phase synchronization errors $\varphi_e(t)$ from the synchronization signal is depicted in **Figure 3**. Firstly,

the pulse-to-pulse phase modulation applied to the synchronization signal during transmission is removed from the overlapped signal, which is the sum of the radar echo and the synchronization signal. Consequently, the Doppler spectrum of the synchronization signal will be shifted at a Doppler frequency equal to

$$f_{Dopp} = \delta f - \frac{v_{Tx-Rx}}{c}\left(2f_{0_{Tx}} + \Delta f\right), \quad (3)$$

where $f_{0_{Tx}}$ is the carrier frequency of the Tx satellite, c is the speed of light, and v_{Tx-Rx} is the relative velocity between the two satellites. Moreover, the spectrum of the synchronization signal does not exhibit a pronounced peak at f_{Dopp} but is be spread across different cells in range and Doppler due to the varying distance between the Tx and Rx satellites during the data take. To address this, following the removal of the phase modulation, compensation for satellite distance variation is applied to the data in the range-frequency-time-azimuth domain by exploiting prior information from orbital data. At this stage, the synchronization signal in the range-Doppler domain, after the range compression, presents a distinct peak at the f_{Dopp} as defined in (3). To shift the spectra of the synchronization signal at Doppler zero, the f_{Dopp} component is removed from the data. The estimation of the frequency offset δf of the two oscillators, i.e., the first component of the f_{Dopp} in (3), relies on the use of the first pulses containing only the synchronization signal. Orbital data is then employed to retrieve the second component of the f_{Dopp} in (3). It is important to note that dual-frequency Global Navigation Satellite System receivers on both satellites and ground-based orbit determination systems can provide accuracy on the order of a few millimetres per second (1-sigma) for the relative velocity between the two satellites. This accuracy level allows us to determine the second component of f_{Dopp} in (3) with an accuracy of less than 1 Hz for an X-band SAR system. Afterwards a narrow range-Doppler filter will be employed around Doppler zero. The extracted synchronization signal is transformed back into the azimuth time domain and the phase of the compressed peak for each pulse is estimated, assuming a constant phase within the main lobe. It can be shown that the phase of the peak is:

$$\varphi_{peak}(t) = M\varphi_{st_{Tx}}(t) - M\varphi_{st_{Rx}}(t - \Delta t_{Rx-Tx}) + \varphi_{re}(t), \quad (4)$$

where $\varphi_{re}(t)$ is the phase of the remaining radar echo component within the range-Doppler filter. After some integration along different pulses the phase errors due to the two independent oscillators are estimated.

Following this, the estimated phase errors are corrected in the received radar echo data, which is overlapped with the synchronization signal before the focusing process. The synchronization signal is subsequently eliminated through azimuth focusing due to the phase modulation, causing the synchronization signal to shift beyond the processed Doppler bandwidth. It is crucial to emphasize that when opting for this phase modulation during transmission to displace the synchronization signal outside the processed Doppler bandwidth, a rough priori knowledge of the Doppler component due to the relative velocity between the two satellites and the frequency offset from the oscillators is necessary. **Figure 4** (a) shows the relative velocity between the HRWS satellite (i.e., Tx satellite) and the three Rx satellites as a function of the argument of latitude for the HRWS mission proposal [9]. We note that the satellite distance variation is less than 1.5 m/s. **Figure 4** (b) shows the corresponding Doppler component as function of the argument of latitude and we note a Doppler frequency variation of 200 Hz within 90 minutes.

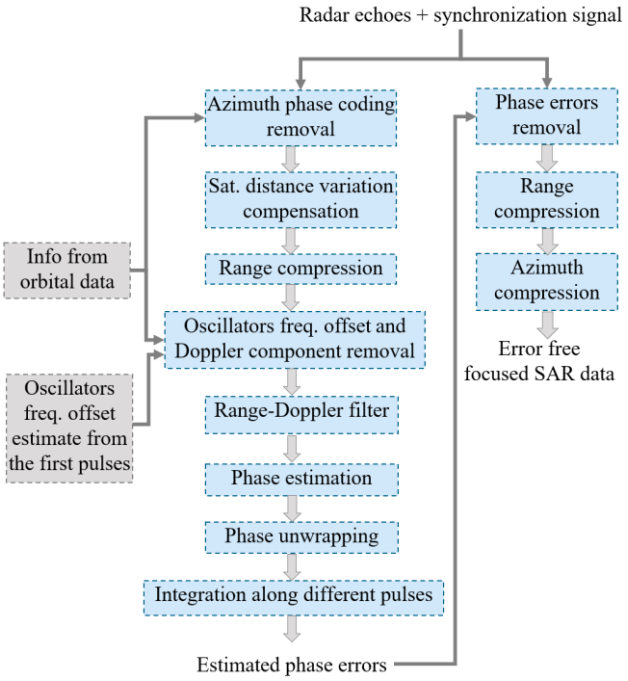

Figure 3 Block diagram of the estimation of the synchronization phase errors from the synchronization signal and synchronization signal removal.

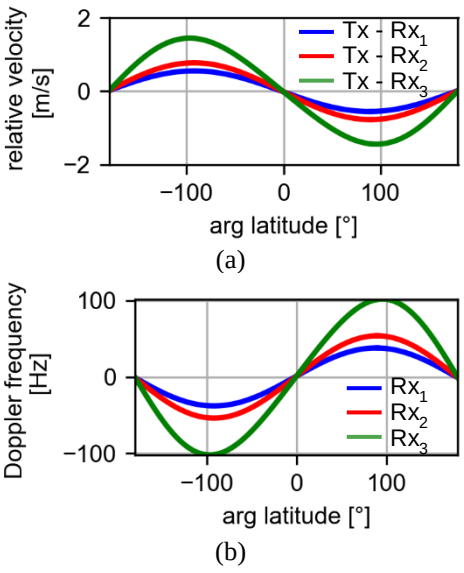

Figure 4 (a) Relative velocity between the Tx and Rx satellites as function of the argument of latitude for the HRWS mission and (b) corresponding Doppler frequency variation as function of the argument of latitude.

It is important to note that although only one Rx satellite is illustrated in **Figure 2** for simplicity, the proposed synchronization scheme can simply be generalized to the case of several Rx satellites. The frequency shift $+\Delta f$ will be different for each Rx satellite in order to avoid interference between the radar echoes from the different satellites. The transmitting satellite may have a larger bandwidth in order to accommodate the radar echoes received by all the Rx satellites.

3 End-to-End Simulation with TanDEM-X Data

In this section, we present an end-to-end simulation of the proposed synchronization scheme using TanDEM-X data. **Figure 5** (a) and (b) display the coherence and the TanDEM-X interferogram acquired over Franz Josef Land, Russia, which we have taken into consideration. We assume that the two images were acquired by two Rx satellites, Rx_1 and Rx_2, respectively. Their relative velocities with respect to the Tx satellite are in the order of 1.5 m/s for Rx_1 and 0.8 m/s for Rx_2, as indicated in the results shown in **Figure 4**. We generated two synchronization signals, assumed to be up-chirp signals, with a 20 µs pulse length, 100 MHz chirp bandwidth, and synchronization signal-to-radar echo ratios of -8 dB. These signals were superimposed to the pair of raw data. Both synchronization signals were phase-modulated to be shifted outside the processed Doppler bandwidth of 2000 Hz. For the frequency shift of $+\Delta f$ by the receiving satellites, we assumed the use of the same ultrastable oscillator of 10 MHz as described in [4]. The same oscillator was considered also for the reversing, i.e., $-\Delta f$, from the Tx satellite (see upper panel in **Figure 2**). We considered different values of Δf for the two satellites: Δf =1.9 GHz for Rx_1 and Δf =1.6 GHz for Rx_2. The synchronization approach on the ground, as illustrated in **Figure 3**, was then applied separately to the two images. **Figure 6** compares the phase errors estimated from the peak phase (shown in blue), without applying a range-Doppler filter to the data, with the simulated phase errors (shown in red) for a synchronization signal-to-radar echo ratio of -8 dB. The estimated phase errors are integrated across different pulses. In **Figure 7** the blue curve illustrates the accuracy of phase error estimation as a function of the integrated pulses for the main image. Notably, for a synchronization signal-to-radar echo power ratio of -8 dB, an accuracy of approximately 0.4° is achieved after integrating 270 pulses. In **Figure 6** the estimated phase errors after integrating 270 pulses (shown in green) are compared with the simulated phase errors (shown in red). Similar results are obtained for the other image, although they are not presented here for brevity. The estimated phase errors were then removed from both the master and slave images before SAR processing. **Figure 5** (c) shows the residual phase errors in the interferometric phase, and we note that the overall remaining phase errors are below 1° for the high coherence areas. We repeat the same steps for the case when the synchronization signal is an up chirp while the signal transmitted to the ground is a down chirp. The accuracy of phase error estimation, as a function of the integrated pulses, is compared to the previous case in **Figure 7** (shown as the dashed red curve). We achieve better accuracy, specifically 0.29°, after integrating 160 pulses.

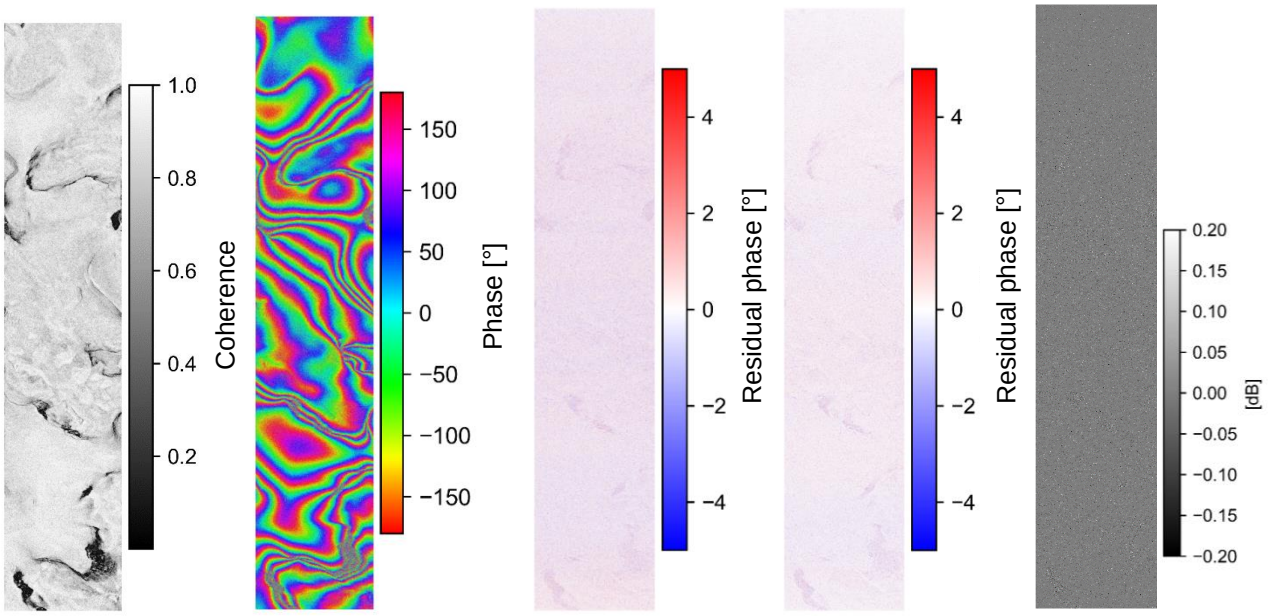

Figure 5 (a) Magnitude of the complex coherence of a TanDEM-X interferogram, acquired over the Franz Josef Land, Russia, (b) interferometric phase, (c) residual phase errors on the interferometric phase after the synchronization when the synchronization signal and the signal transmitted to the ground are both up-chirps (d) residual phase errors on the interferometric phase after the synchronization when the synchronization signal is a down-chirp and the signal transmitted to the ground is an up-chirp and (e) difference in amplitude between the main image after the removal of the synchronization signal and the main original data.

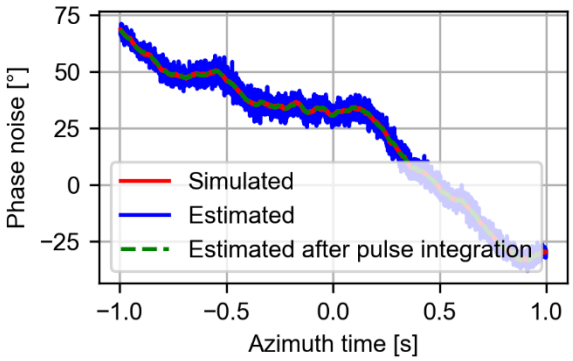

Figure 6 Comparison between the estimated phase error before and after the integration of 270 pulses and the simulated phase error when the synchronization signal-to-radar echo ratio is – 8 dB.

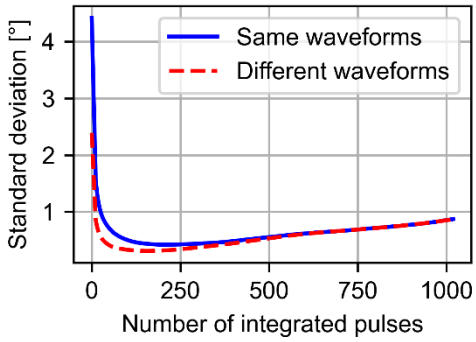

Figure 7 Phase noise estimation accuracy as function of the number of integrated pulses.

Figure 5 (d) displays the residual phase errors in the interferometric phase for this scenario, and it is noticeable that the overall remaining phase errors are below to those in **Figure 5** (c). This improvement is due to the mismatch during range compression, which results in a smeared radar echo proportional to the range compression ratio.
Finally, during the SAR processing of the phase-corrected images, a Doppler bandwidth of 2000 Hz was processed, and the synchronization signal was removed as it fell outside of the processed bandwidth. **Figure 5** (e) shows the difference between the main image after the removal of the synchronization signal and the original main data. We observe errors below 0.05 dB.

4 Conclusions

In this paper, we investigated a phase synchronization technique based on microwave links within the MirrorSAR concept. The accuracy of the proposed technique has been evaluated through simulations using TanDEM-X data. We demonstrated that even when the synchronization signal-to-radar echo ratio is as low as -8 dB, the proposed synchronization technique guarantees phase error estimations with an accuracy of less than 1°. Additionally, we showed that the synchronization signal as it was shifted outside the processed Doppler bandwidth, had no impact on the radar echo data.

Acknowledgment

This work was partially funded by the European Union (ERC, DRITUCS, 101076275). Views and opinions expressed are however those of the authors only and do not necessarily reflect those of the European Union or the European Research Council Executive Agency. Neither the European Union nor the granting authority can be held responsible for them.

5 Literature

[1] G. Krieger and A. Moreira, “Bi- and multi-static SAR: Potentials and challenges,” *Proc. Inst. Electr. Eng.—Radar Sonar Navig.*, vol. 153, no. 3, pp. 184–198, Jun. 2006.

[2] J. Ender, I. Walterscheid, and A. Brenner, “New aspects of bistatic SAR: Processing and experiments,” in *Proc. IGARSS*, Anchorage, AK, 2004, pp. 1758–1762.

[3] J. L. Auterman, “Phase stability requirements for a bistatic SAR,” *in Proc. IEEE Nat. Radar Conf.*, Atlanta, GA, 1984, pp. 48–52.

[4] G. Krieger and M. Younis, “Impact of oscillator noise in bistatic and multistatic SAR,” *IEEE Geoscience and Remote Sensing Letters*, vol. 3, no. 3, pp. 424-428, July 2006.

[5] M. Eineder, “Oscillator clock drift compensation in bistatic interferometric SAR,” in Proc. IGARSS, Toulouse, France, 2003, pp. 1449–1451.

[6] M. Younis, R. Metzig and G. Krieger, "Performance prediction of a phase synchronization link for bistatic SAR," IEEE Geoscience and Remote Sensing Letters, vol. 3, no. 3, pp. 429-433, July 2006.

[7] G. Krieger *et al.*, “TanDEM-X: A Satellite Formation for High-Resolution SAR Interferometry,” *IEEE Transactions on Geoscience and Remote Sensing*, vol. 45, no. 11, pp. 3317-3341, Nov. 2007.

[8] G. Krieger et al., “MirrorSAR: A fractionated space radar for bistatic, multistatic and high-resolution wide-swath SAR imaging,” 2017 IEEE International Geoscience and Remote Sensing Symposium (IGARSS), 2017, pp. 149-152.

[9] J. Mittermayer et al., “MirrorSAR: An HRWS Add-On for Single-Pass Multi-Baseline SAR Interferometry,” *IEEE Transactions on Geoscience and Remote Sensing*, vol. 60, pp. 1-18, 2022.

[10] P. Lopez-Dekker, J. J. Mallorqui, P. Serra-Morales and J. Sanz-Marcos, “Phase Synchronization and Doppler Centroid Estimation in Fixed Receiver Bistatic SAR Systems,” *IEEE Transactions on Geoscience and Remote Sensing*, vol. 46, no. 11, pp. 3459-3471, Nov. 2008.

[11] E. Loria, S. Prager, I. Seker, R. Ahmed, B. Hawkins and M. Lavalle, "Modeling the Effects of Oscillator Phase Noise and Synchronization on Multistatic SAR Tomography," in *IEEE Transactions on Geoscience and Remote Sensing*, vol. 61, pp. 1-12, 2023.